

doi: 10.15407/ujpe62.08.0653

K.A. HUSSAIN,<sup>1</sup> M.K. MOHSIN,<sup>1</sup> F.I. SHARRAD<sup>2</sup>

<sup>1</sup> Department of Physics, College of Science, University of Babylon  
(51002Hilla, Iraq.)

<sup>2</sup> Department of Physics, College of Science, University of Kerbala  
(56001 Karbala, Iraq.; e-mail: fadhil.altaie@gmail.com)

PACS 21.60.Ev, 27.70.+q,  
23.20.-g, 23.20.Lv,  
21.10.-k, 42.40.Ht,  
42.30.Kq

## CALCULATION OF THE POSITIVE PARITY YRAST BANDS OF <sup>190–198</sup>Hg NUCLEI

---

*The Interacting Boson Model (IBM-1) has been used to calculate the low-lying positive parity yrast bands in <sup>190–198</sup>Hg nuclei. The systematic yrast level and electric reduced transition probabilities  $B(E2)_{\downarrow}$  of those nuclei are calculated and compared with the available experimental data. The ratio of the excitation energies of first  $4^+$  and first  $2^+$  excited states,  $R_{4/2}$ , is also studied for the  $O(6)$  symmetry for these nuclei. Furthermore, as a measure to quantify the evolution, we have studied systematically the yrast level  $R = E_{L_1^+}/E_{2_1^+}$  of some of the low-lying quadrupole collective states in comparison to the available experimental data. Moreover, we have studied the systematic  $B(E2)$  values, and the moment of inertia as a function of the squared rotational energy for even proton  $Z = 80$  and  $110 \leq N \leq 118$  nuclei indicates the disappearance of back-bending properties. The results of this calculation are in good agreement with the corresponding available experimental data. The analytic IBM-1 calculation of the yrast level and  $B(E2)$  values of even-even Hg nuclei is performed in the framework of  $O(6)$  symmetry. The contour plot of the potential energy surfaces shows that the nuclei are deformed and have  $\gamma$ -unstable-like characters.*

*Keywords:* IBM-1,  $B(E2)$  values, energy levels, potential energy.

### 1. Introduction

The mercury nuclei are situated in a transition region, which lies above the region of the deformed prolate rare earth nuclei and just below the spherical lead nuclei at  $Z = 82$  [1]. These nuclei are characterized by changes between the spherical and deformed shapes [2]. In calculations within the Interacting Boson Model (IBM-1), these nuclei have been successfully treated as exhibiting the  $O(6)$  symmetry [3] of this model. The IBM [4] has been successful in reproducing the nuclear collective levels in terms of  $s$  and  $d$  bosons, which are essentially the collective  $s$  and  $d$  pairs of valence nucleons [5], respectively. As the  $s$  and  $d$  bosons span a six-dimensional Hilbert space, the Hamiltonian corresponding to the IBM-1

has a group structure  $U(6)$ . The three limiting symmetries of this Hamiltonian,  $U(2)$ ,  $SU(3)$ , and  $O(6)$ , correspond to the geometrical shapes of a spherical vibrator and a symmetric rotor and to the  $\gamma$ -instability, respectively [6, 7].

The application of this model to deformed and vibrating nuclei is currently a subject of considerable interest and controversy. Here, we apply the IBM model to account for even-even mercury isotopes. The detailed work on the structure of mercury nuclei was done in recent years. The collective nuclear structure of light- and medium-mass atomic nuclei have been studied by the energy level structures of the ground band in the first instance, and the nuclear structure was discussed with the use of the observables of collectivity and deformation [8]. The structure of high-spin states in the transitional nuclei <sup>190,192,194</sup>Hg was

described in the framework of the interacting boson model with one and two broken pairs [9]. The ground states of Hg and Pb isotopes in the framework of the deformed relativistic mean field theory with pairing interactions in the BCS theory and the oblate shape and the charge radius of neutron-deficient Hg isotopes were well reproduced [10]. The average  $g$  factors of high spin, high-excitation energy, and quasicontinuum structures in  $^{194,193}\text{Hg}$  have been measured, by observing the precessions of the angular distributions of gamma-ray transitions in several normal-deformation bands that coalesce in the decay of the entry distribution of states [11]. Nomura *et al.* [12] applied the interacting boson model with configuration mixing and with parameters derived from the self-consistent mean-field calculation employing the microscopic Gogny energy density functional to the systematic analysis of the low-lying structure in Hg isotopes. Bernards *et al.* [13] studied  $0^+$  states in  $^{198}\text{Hg}$  after the  $^{200}\text{Hg}(p, t)^{198}\text{Hg}$  transfer reaction up to the 3-MeV excitation energy, and the experiment was performed, by using a high-resolution Q3D magnetic spectrograph at the Maier–Leibnitz Laboratory Tandem accelerator in Munich. García–Ramos *et al.* [14] described the even-even Hg isotopes,  $^{172-200}\text{Hg}$ , by using the interacting boson model including the configuration mixing and paid a special attention to the description of the shape of nuclei and to its connection with the shape coexistence phenomenon. The electromagnetic properties of radioactive even-even Hg isotopes were performed with 2.85 MeV nucleon mercury beams from REX–ISOLDE and extracted the magnitudes and relative signs of the reduced  $E2$  matrix elements that couple the ground state and low-lying excited states in  $^{182-188}\text{Hg}$  in view of Coulomb-excitation experiments [15].

The bulk and decay properties, including the deformation energy curves, charge mean square radii Gamow–Teller (GT) strength distributions, and  $\beta$ -decay half-life in neutron-deficient even-even and odd- $A$  Hg and Pt isotopes had been studied. From the calculations in the deformed quasiparticle random-phase approximation with residual interactions in both particle-hole and particle-particle channels, which were performed on the top of a self-consistent deformed quasiparticle Skyrme–Hartree–Fock basis, the nuclear structure was described microscopically in [16].

In the same region of Hg isotopes, the evolution properties of the yrast states and the electromagnetic

reduced transition probabilities for even-even Pt isotopes were studied in [4, 17–19] within the framework of the interesting boson model

## 2. Interacting Boson Model (IBM-1)

The IBM-1 of Arima and Iachello [20] has become widely accepted as a tractable theoretical scheme of correlating, describing, and predicting low-energy collective properties of complex nuclei. In the IBM, the spectroscopies of low-lying collective properties of even-even nuclei were described in terms of a system of interacting  $s$  bosons ( $L = 0$ ) and  $d$  bosons ( $L = 2$ ) [17, 21]. In the original form of the model known as IBM-1, proton and neutron-boson degrees of freedom are not distinguished. The model has an inherent group structure associated with it. The IBM-1 Hamiltonian can be expressed as [22, 23]

$$\begin{aligned}
 H = & \varepsilon_s (s^\dagger \tilde{s}) + (d^\dagger \tilde{d}) + \\
 & + \sum_{L=0,2,4} \frac{1}{2} (2L+1)^{\frac{1}{2}} C_L \left[ [d^\dagger \times d^\dagger]^{(L)} \times [\tilde{d} \times \tilde{d}]^{(L)} \right]^{(0)} + \\
 & + \frac{1}{\sqrt{2}} v_2 \left[ [d^\dagger \times d^\dagger]^{(2)} \times [\tilde{d} \times \tilde{s}]^{(2)} + \right. \\
 & \left. + [d^\dagger \times s^\dagger]^{(2)} \times [\tilde{d} \times \tilde{d}]^{(2)} \right]^{(0)} + \\
 & + \frac{1}{2} v_0 \left[ [d^\dagger \times d^\dagger]^{(0)} \times [\tilde{s} \times \tilde{s}]^{(0)} + \right. \\
 & \left. + [s^\dagger \times s^\dagger]^{(0)} \times [\tilde{d} \times \tilde{d}]^{(0)} \right]^{(0)} + \\
 & + \frac{1}{2} u_0 \left[ [s^\dagger \times s^\dagger]^{(0)} \times [\tilde{s} \times \tilde{s}]^{(0)} \right]^{(0)} + \\
 & + u_2 \left[ [d^\dagger \times s^\dagger]^{(2)} \times [\tilde{d} \times \tilde{s}]^{(2)} \right]^{(0)}. \tag{1}
 \end{aligned}$$

This Hamiltonian contains two terms of one-body interactions, ( $\varepsilon_s$  and  $\varepsilon_d$ ), and seven terms of two-body interactions [ $c_L(L = 0, 2, 4)$ ,  $v_L(L = 0, 2)$ ,  $u_L(L = 0, 2)$ ], where  $\varepsilon_s$  and  $\varepsilon_d$  are the single-boson energies, and  $c_L$ ,  $v_L$ , and  $u_L$  describe the two-boson interactions. However, it turns out that, for a fixed boson number  $N$ , only one of the one-body terms and five of the two-body terms are independent, as it can be seen by noting  $N = n_s + n_d$ . Equation (1) can be rewritten in terms of the Casimir operators of the U(6) group. The O(6) symmetry of the IBM-1 is based on the chain U(6)  $\supset$  O(6)  $\supset$  O(2)  $\supset$  O(3) of nested subalgebra with quantum numbers  $N$ ,  $\sigma$ ,  $\tau$ , and  $L$ , respectively [22–24].

Table 1. Parameters used for IBM-1 calculations. All parameters are given in MeV except for  $N$  and  $\text{CHQ}(\chi)$

Nucl.	$N_\pi + N_\nu = N$	$\varepsilon$	$\alpha_0$	$\alpha_1$	$\alpha_2$	$\alpha_3$	$\alpha_4$	$\text{CHQ}(\chi)$
$^{190}\text{Hg}$	$1 + 8 = 9$	0.000	0.1279	0.0179	0.000	0.2206	0.000	0.000
$^{192}\text{Hg}$	$1 + 7 = 8$	0.000	0.1408	0.0183	0.000	0.2234	0.000	0.000
$^{194}\text{Hg}$	$1 + 6 = 7$	0.000	0.1875	0.0210	0.000	0.2159	0.000	0.000
$^{196}\text{Hg}$	$1 + 5 = 6$	0.000	0.1884	0.0264	0.000	0.1902	0.000	0.000
$^{198}\text{Hg}$	$1 + 4 = 5$	0.000	0.2336	0.0186	0.000	0.2143	0.000	0.000

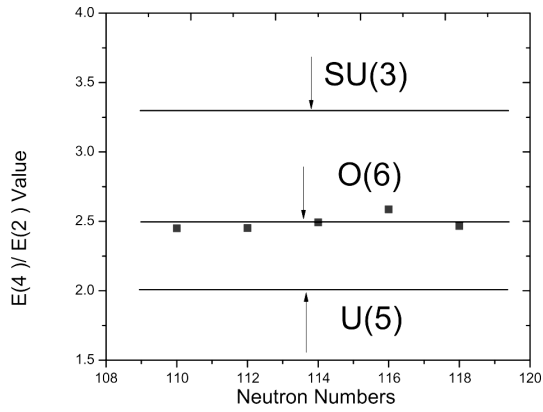


Fig. 1.  $E4_1^+/E2_1^+$  values of low-lying energy levels of  $^{190-198}\text{Hg}$  nuclei

Then the IBM-1 Hamiltonian in Eq. (1) can be written in the general form as [24, 25]:

$$\hat{H} = \varepsilon \hat{n}_d + \alpha_0 \hat{P} \cdot \hat{P} + \alpha_1 \hat{L} \cdot \hat{L} + \alpha_2 \hat{Q} \cdot \hat{Q} + \alpha_3 \hat{T}_3 \cdot \hat{T}_3 + \alpha_4 \hat{T}_4 \cdot \hat{T}_4, \quad (2)$$

where:  $\hat{n}_d = (s^\dagger, d^\dagger)$  is the total number of  $d_{\text{boson}}$  operators,  $\hat{p} = 1/2[(\tilde{d} \cdot \tilde{d}) - (\tilde{s} \cdot \tilde{s})]$  is the pairing operator,  $\hat{L} = \sqrt{10}[d^\dagger \times \tilde{d}]^1$  is the angular momentum operator,  $\hat{Q} = [d^\dagger \times \tilde{s} + s^\dagger \times \tilde{d}]^{(2)} + \chi[d^\dagger \times \tilde{d}]^{(2)}$  is the quadrupole operator ( $\chi$  is the quadrupole structure parameter and takes the values 0 and  $\pm\sqrt{7}$ ),  $\hat{T}_r = [d^\dagger \times \tilde{d}]^{(r)}$  presents the octupole ( $r = 3$ ) and hexadecapole ( $r = 4$ ) operators, and  $\varepsilon = \varepsilon_d - \varepsilon_s$  is the boson energy.

The parameters  $a_0$ ,  $a_1$ ,  $a_2$ ,  $a_3$ , and  $a_4$  designate the strength of the pairing, angular momentum, quadrupole, and octupole and hexadecapole interactions between the bosons.

### 3. Results and Discussion

The Hg nuclei have the proton number equal to 80 and the neutron numbers 110, 112, 114, 116, and

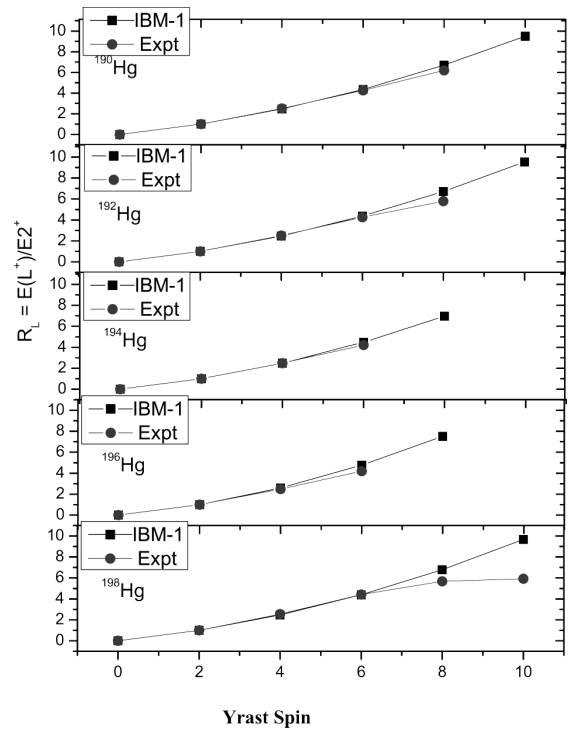


Fig. 2. Comparison of the ratios  $R_L = E(L^+)/E(2_1^+)$  as functions of the angular momentum ( $L$ ) in the yrast band for the nuclei

118. According to the IBM-1, the numbers of neutron boson holes 8, 7, 6, 5, and 4, and there is one proton hole. The total numbers of bosons are 9, 8, 7, 6, and 5 of  $^{190-198}\text{Hg}$  nuclei. The symmetry shape of a nucleus can be predicted from the energy ratio  $R = E4_1^+/E2_1^+$ , where  $E4_1^+$  is the energy level at  $4_1^+$ , and  $E2_1^+$  is the energy level at  $2_1^+$ . Actually,  $R$  has a limit value of  $\approx 2$  for the vibration nuclei [U(2) symmetry],  $\approx 2.5$  for  $\gamma$ -unstable nuclei [O(6) symmetry], and  $\approx 3.33$  for rotational nuclei [SU(3) symmetry] [24]. The  $R$  values of low-lying energy levels of

Table 2. Comparison of theoretical and experimental [26–31] excitation energies (in units of MeV) of  $^{190-198}\text{Hg}$  nuclei

Nucl.	$E(2_1^+)$	$E(4_1^+)$	$E(4_1^+)/E(2_1^+)$	$E(2_1^+)$	$E(4_1^+)$	$E(4_1^+)/E(2_1^+)$
$^{190}\text{Hg}$	0.41632	1.02002	2.45008	0.41632	1.04177	2.50232
$^{192}\text{Hg}$	0.42279	1.03695	2.45263	0.42279	1.05758	2.50143
$^{194}\text{Hg}$	0.42796	1.06674	2.49261	0.42789	1.06419	2.48706
$^{196}\text{Hg}$	0.42454	1.09815	2.58668	0.42598	1.06144	2.49176
$^{198}\text{Hg}$	0.41180	1.01550	2.46600	0.41180	1.04849	2.54611

Table 3. Reduced transition probability  $B(E2) \downarrow$  in even  $^{190-198}\text{Hg}$  nuclei

Nucl	$\alpha$ e.b	Yrast level	Energy (MeV)	Transition level	$B(E2)$ exp. $e^2 \cdot b^2$	$B(E2)$ IBM-1 $e^2 \cdot b^2$
$^{190}\text{Hg}$	04503	2	0.41632	$2^+ \rightarrow 0^+$	–	0.0474
		4	0.6037	$4^+ \rightarrow 2^+$	–	0.0649
		6	0.79107	$6^+ \rightarrow 4^+$	–	0.0710
		8	0.97846	$8^+ \rightarrow 6^+$	–	0.0708
		10	1.16584	$10^+ \rightarrow 8^+$	–	0.0663
		12	1.35323	$12^+ \rightarrow 10^+$	–	0.0584
$^{192}\text{Hg}$	08009	2	0.42279	$2^+ \rightarrow 0^+$	–	0.1232
		4	0.61416	$4^+ \rightarrow 2^+$	–	0.1668
		6	0.800556	$6^+ \rightarrow 4^+$	–	0.1796
		8	0.99693	$8^+ \rightarrow 6^+$	–	0.1750
		10	1.18832	$10^+ \rightarrow 8^+$	0.157906	0.1579
		12	1.3797	$12^+ \rightarrow 10^+$	0.12500	0.1309
$^{194}\text{Hg}$	10931	2	0.42796	$2^+ \rightarrow 0^+$	–	0.1840
		4	0.63878	$4^+ \rightarrow 2^+$	–	0.2458
		6	0.8496	$6^+ \rightarrow 4^+$	–	0.2589
		8	1.06043	$8^+ \rightarrow 6^+$	–	0.2433
		10	1.27125	$10^+ \rightarrow 8^+$	0.206799	0.2068
		12	1.48207	$12^+ \rightarrow 10^+$	0.160103	0.1529
$^{196}\text{Hg}$	13699	2	0.42454	$2^+ \rightarrow 0^+$	0.225201	0.2252
		4	0.67361	$4^+ \rightarrow 2^+$	–	0.2949
		6	0.92268	$6^+ \rightarrow 4^+$	–	0.3003
		8	1.17175	$8^+ \rightarrow 6^+$	–	0.2661
		10	1.42082	$10^+ \rightarrow 8^+$	0.229935	0.2021
		12	1.66989	$12^+ \rightarrow 10^+$	–	–
$^{198}\text{Hg}$	14811	2	0.4118	$2^+ \rightarrow 0^+$	0.1974	0.1974
		4	0.6037	$4^+ \rightarrow 2^+$	–	0.2507
		6	0.7956	$6^+ \rightarrow 4^+$	–	0.2413
		8	0.9875	$8^+ \rightarrow 6^+$	–	0.1914
		10	1.1794	$10^+ \rightarrow 8^+$	–	–
		12	–	$12^+ \rightarrow 10^+$	–	–

$^{190-198}\text{Hg}$  nuclei are 2.50, 2.50, 2.48, 2.49, and 2.54, respectively, which are shown in Fig. 1. From this figure, we have predicted the O(6) symmetry for even-even  $^{190-198}\text{Hg}$  nuclei.

### 3.1. Yrast levels

The yrast levels (2, 4, 6, 8, and 10) of  $^{190-198}\text{Hg}$  nuclei have been calculated by taking the number of free parameters in the Hamiltonian to be minimum. These

parameters are determined from the experimental energy levels ( $2^+$  and  $4^+$ ). Each nucleus at the evolving states is described, by using Eq. (2).

Table 1 shows the IBM-1 parameters that are used in the calculations of yrast states of those nuclei. All parameters are given in MeV except for  $N$  and  $\text{CHQ}(\chi)$ . Table 2 shows comparisons of theoretical and experimental excitation energies (in units of MeV) up to  $1^{\text{st}}$   $4^+$  levels, and their ratio  $R = E4_1^+/E2_1^+$  gives the energy level fit, as well as rotational and gamma soft nuclear deformations.

Figure 2 demonstrates the comparison of the ratios  $R_L = E(L^+)/E(2_1^+)$  as functions of the angular momentum ( $L$ ) in the yrast band for those nuclei. To measure the evolution of the nuclei collectively, we present the energies of the yrast sequences within the IBM-1 (normalized to the energy of their respective  $2_1^+$  levels) in the nuclei and have compared with previous experimental values [26–31].

From Fig. 2, we can see that the IBM-1 calculation fits the O(6)-based predictions. The comparison of the results of calculations and the experimental values shows the excellent agreement, and  $R_L$  increases toward higher spin states. The  $R_L$  values of  $^{190-198}\text{Hg}$  nuclei indicate that their excitations are similar and have a lower value of  $R_L$  because of the O(6) symmetry.

### 3.2. Reduced Transition Probabilities $B(E2)$

The low-lying levels of even-even nuclei ( $L_i = 2, 4, 6, 8, 10,$  and  $12$ ) usually decay by one  $E2$  transition to the lower-lying yrast level with  $L_f = L_i - 2$ . The reduced transition probabilities in the IBM-1 are given for the anharmonic vibration limit within O(6) as [4, 23, 24]

$$B(E2; L+2 \rightarrow L) \downarrow = \alpha_2^2 \frac{L+2}{8(L+5)} (2N-L)(2N+L+8), \quad (3)$$

where  $L$  is the angular momentum, and  $N$  is the boson number, which is equal to half the number of valence nucleons (proton and neutrons). From the given experimental value  $B(E2)$  of transition ( $L+2 \rightarrow L$ ), one can calculate the value of the parameter  $\alpha_2^2$  for each isotope, where  $\alpha_2^2$  indicates the squared effective charge. This value is used to calculate the reduced transition probabilities  $B(E2; L+2 \rightarrow L) \downarrow$ . Table 3 indicates the reduced transition probabilities for all nuclei and the excellent agreement of the calculated

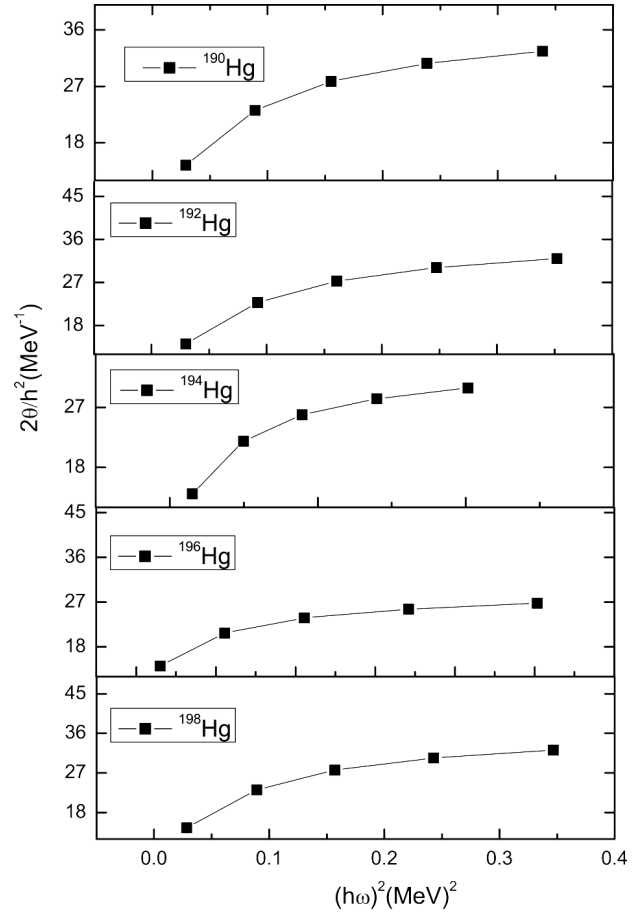


Fig. 3. The moment of inertia  $2\vartheta/\hbar^2$  as a function of  $(\hbar\omega)^2$

values with the experimental data. It is shown that  $B(E2)$  values are maximum for the transition ( $8^+$  to  $6^+$ ) in each nuclei. Moreover, the reduced transition probabilities decrease, as the neutron number increases toward the shell  $N = 126$ .

### 3.3. Back-bending

The positive parity yrast levels are connected by a sequence of stretched  $E2$  transitions with energies, which increase smoothly except for around the backbends. The transition energy  $\Delta E_{I, I-2}$  should increase linearly with  $I$  for the constant rotor as  $\Delta E_{I, I-2} = I/2\vartheta(4I-2)$  does not increase, but decreases for certain  $I$  values. The relation between the moment of inertia ( $\vartheta$ ) and the gamma energy  $E_\gamma$  is given by

$$2\vartheta/\hbar^2 = \frac{2(2I-1)}{E(I) - E(I-2)} = \frac{4I-2}{E_\gamma}, \quad (4)$$

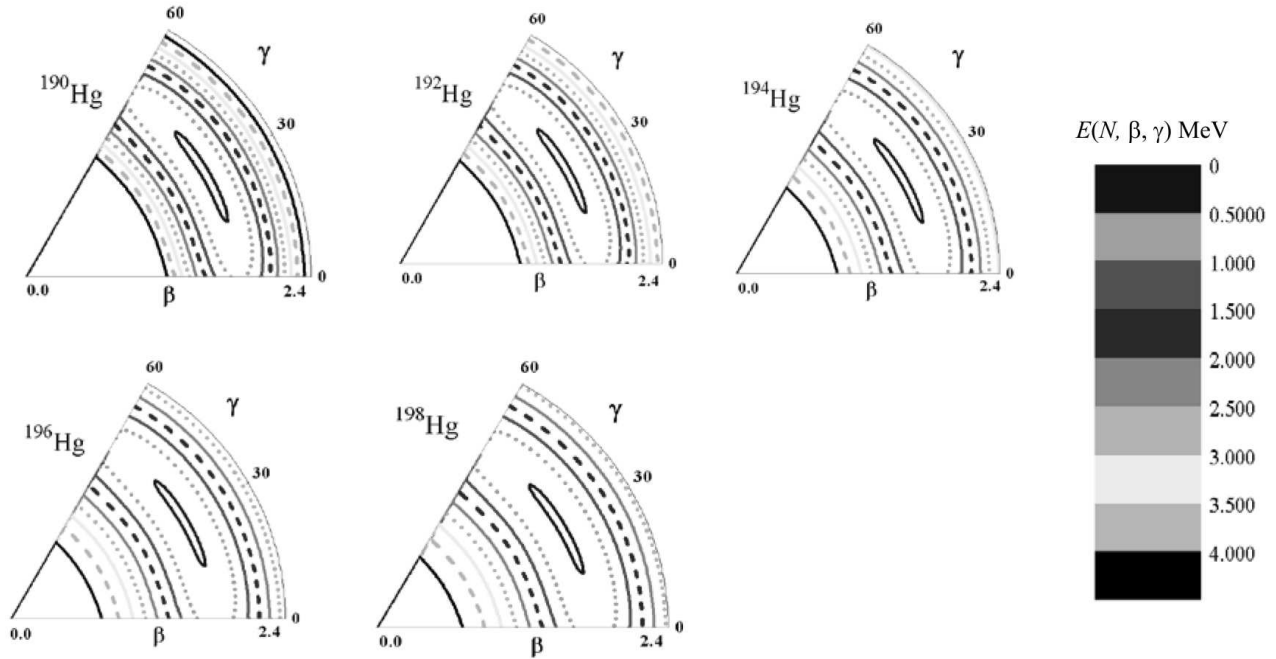


Fig. 4. The potential energy surface in the  $\gamma\beta$  lane for  $^{190-198}\text{Hg}$  nuclei

and the relation between  $E_\gamma$  and  $\hbar\omega$  is given by

$$\begin{aligned} \hbar\omega &= \frac{E(I) - E(I-2)}{\sqrt{I(I+1)} - \sqrt{(I-2)(I-1)}} = \\ &= \frac{E_\gamma}{\sqrt{I(I+1)} - \sqrt{(I-2)(I-1)}}. \end{aligned} \quad (5)$$

The moment of inertia  $2\vartheta/\hbar^2$  and the rotational frequency  $\hbar\omega$  have been calculated from Eqs. (4) and (5), respectively. The ground-state bands up to 10 units of angular momentum are investigated with regard for the moment of inertia in Hg isotopes. The moments of inertia are plotted versus the squared rotational energy in Fig. 3. Usually, in the lowest order according to the variable moment of inertia (VMI) model, this should give a straight line in the plot of the inertia  $2\vartheta/\hbar^2$  as a function of  $(\hbar\omega)^2$ . There is no back-bending for Hg nuclei. The back-bending phenomena disappear clearly in the diagram  $2\vartheta/\hbar^2$  vs  $(\hbar\omega)^2$ . The back-bending phenomenon can be phenomenological reproduced as an effect due to the crossing of two bands.

### 3.4. Potential energy surface ( $E(N, \beta, \gamma)$ )

The calculated results can be discussed separately for the potential energy surface ( $E(N, \beta, \gamma)$ ), which

gives a final shape to the nucleus according to the Hamiltonian [23, 24]:

$$E(N, \beta, \gamma) = \frac{\langle N, \beta, \gamma | H | N, \beta, \gamma \rangle}{\langle N, \beta, \gamma | N, \beta, \gamma \rangle}. \quad (6)$$

The expectation value of the IBM-1 Hamiltonian with the coherent state ( $|N, \beta, \gamma\rangle$ ) is used to create the IBM energy surface [23, 24].

The state is a product of boson creation operators ( $b_c^\dagger$ ) with

$$|N, \beta, \gamma\rangle = \frac{1}{\sqrt{N!}} (b_c^\dagger)^N |0\rangle. \quad (7)$$

$$\begin{aligned} b_c^\dagger &= (1 + \beta^2)^{-1/2} \times \\ &\times \left\{ s^\dagger + \beta \left[ \cos \gamma (d_0^\dagger) + \sqrt{\frac{1}{2}} \sin \gamma (d_2^\dagger + d_{-2}^\dagger) \right] \right\}. \end{aligned} \quad (8)$$

The energy surface, as a function of  $\beta$  and  $\gamma$ , is given by [24]

$$\begin{aligned} E(N, \beta, \gamma) &= N\varepsilon_d\beta^2/1 + \beta^2 + N(N-1)/(1 + \beta^2)^2 \times \\ &\times (\alpha_1\beta^4 + \alpha_2\beta^3 \cos 3\gamma + \alpha_3\beta^2 + \alpha_4), \end{aligned} \quad (9)$$

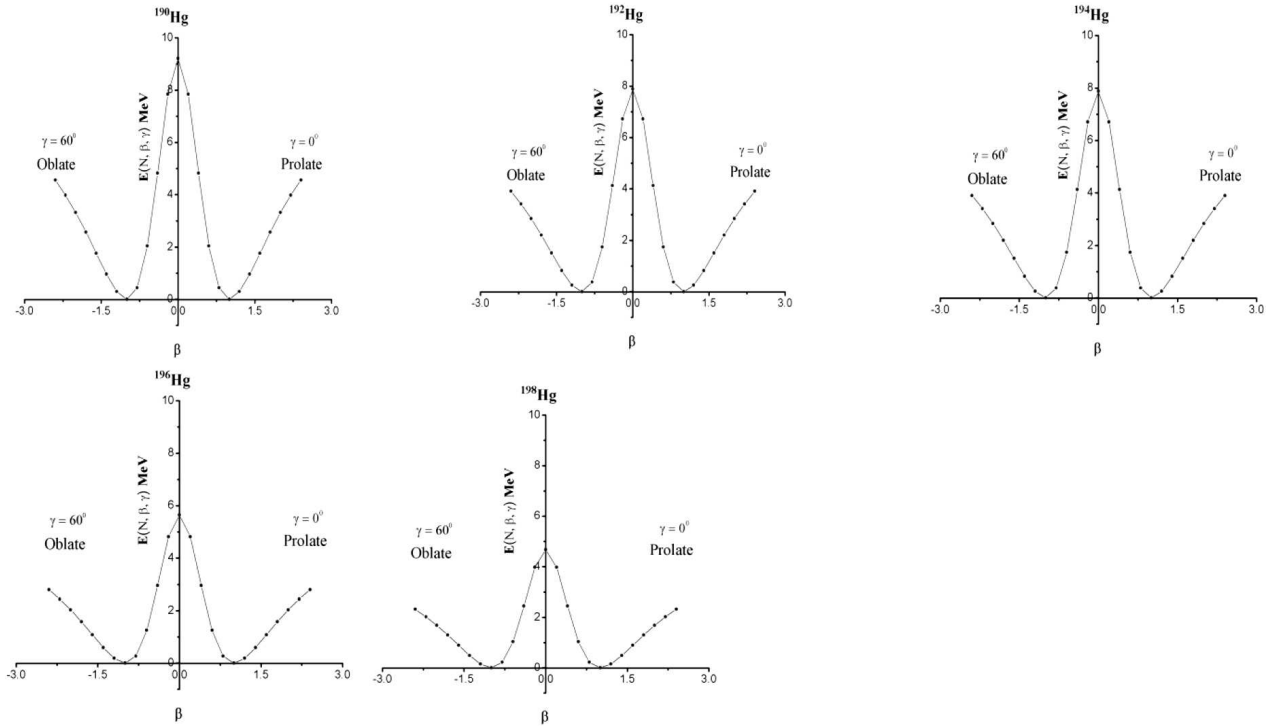


**Fig. 5.** Potential energy surface  $E(N, \beta, \gamma)$  as a function of the deformation parameter for  $^{190-198}\text{Hg}$  isotopes

where the  $\alpha'_i$  are related to the coefficients  $C_L$ ,  $\nu_2$ ,  $\nu$ ,  $u_2$ , and  $u$  of Eq. (1). The quantity  $\beta$  is the measure of a total deformation of the nucleus, where the shape is spherical for  $\beta = 0$  and is distorted if  $\beta \neq 0$ , and  $\gamma$  is the amount of deviation from the focus symmetry and correlates with the nucleus. If  $\gamma = 0$ , the shape is prolate. If  $\gamma = 60$ , the shape becomes oblate. In Fig. 4, the contour plots in the  $\gamma - \beta$  plane resulting from  $E(N, \beta, \gamma)$  are shown for  $^{190-198}\text{Hg}$  isotopes. For most of the considered Hg nuclei, the mapped IBM energy surfaces have triaxial shape. The triaxial shape is associated with intermediate values  $0 < \gamma < \pi/3$ . The triaxial deformation helps to understand the prolate-to-oblate shape transition that occurs in the considered Hg isotopes. The Hg nuclei considered here do not display any rapid structural change, but remain  $\gamma$ -soft. This evolution reflects the triaxial deformation, as one approaches the neutron shell closure  $N = 126$ .

Figure 5 shows the potential energy surface  $E(N, \beta, \gamma)$  as a function of the deformation parameter  $\beta$  with  $\gamma = 0$  and  $60$  for  $^{190-198}\text{Hg}$  isotopes. From this figure, the plane figure shows the symmetry between the potential energy surfaces at  $\gamma = 0$  and  $60$

at  $\beta \sim 1.5$  for the Hg nuclei that are deformed and have the  $\gamma$ -unstable shape.

#### 4. Conclusions

We have reported on the evolution of positive parity yrast levels and reduced transition  $B(E2)$  values for  $^{190-198}\text{Hg}$  nuclei within the IBM-1 and compared with previous experimental values. The predicted low-lying levels and the reduced probabilities are consistent with the experimental results. The back-bending phenomena of those nuclei disappear clearly in the diagram  $2\vartheta/\hbar^2$  vs  $(\hbar\omega)^2$ . The analytic IBM-1 calculation of those values for even-even Hg nuclei with  $N = 110 - 118$  has been performed within the  $O(6)$  symmetry. The results are extremely useful for compiling the nuclear data table. The contour plot of the potential energy surfaces shows that the interested nuclei are deformed and have  $\gamma$ -unstable-like character.

*We thank University of Kerbela-College of Science-Department and University of Babylon-College of Science-Department of Physics for supporting this work.*

1. R.M. Lieder, H. Beuscher, W.F. Davidson, A. Neskakis, C. Mayer-Böricke. Excitation of high-spin states in  $^{190,191,192,193,194}\text{Hg}$  through  $(\alpha, xn)$  reactions. *Nucl. Phys. A* **248**, 317 (1975).
2. A. Sethi, N.M. Hintz, D.N. Mihailidis, A.M. Mack, M. Gazzaly, K. W. Jones, G. Pauletta, L. Santi, D. Goutte. Inelastic proton scattering from Pt isotopes and the interacting boson model. *Phys. Rev. C* **44**, 700 (1991).
3. A. Arima, F. Iachello. Interacting boson model of collective nuclear states IV. The  $O(6)$  limit. *Ann. Phys. NY* **123**, 468 (1979).
4. H.H. Kassim, F.I. Sharrad. Negative parity low-spin states of even-odd  $^{187-197}\text{Pt}$  isotopes. *Nucl. Phys. A* **933**, 1 (2015).
5. T. Otsuka, A. Arima, F. Iachello. Nuclear shell model and interacting bosons. *Nucl. Phys. A* **309**, 1 (1978).
6. F. Iachello, A. Arima. Boson symmetries in vibrational nuclei. *Phys. Lett. B* **53**, 309 (1974).
7. A. Arima, F. Iachello. Collective nuclear states as representations of a  $SU(6)$  group. *Phys. Rev. Lett.* **35**, 1069 (1975).
8. R. Kumar, S. Sharma, J.B. Gupta. Character of quasi-bands in 150 sm using IBM. *Arm. J. Phys.* **3**, 150 (2010).
9. D. Vretenar, G. Bonsignori, M. Savoia. One and two broken pairs in the interacting boson model: High-spin states in  $^{190,192,194}\text{Hg}$ . *Phys. Rev. C* **47**, 2019 (1993).
10. S. Yoshida, N. Takigawa. Shape dependence of pairing gap energies and the structure of Hg and Pb isotopes. *Phys. Rev. C* **55**, 1255 (1997).
11. L. Weissman, R.H. Mayer, G. Kumbartzki, N. Benczer-Koller, C. Broude, J.A. Cizewski, M. Hass, J. Holden, R.V.F. Janssens, T. Lauritsen, I.Y. Lee, A.O. Macchiavelli, D.P. McNabb, M. Satteson. Single particle signatures in high-spin, quasicontinuum states in Hg-193, Hg-194 from  $g$ -factor measurements. *Phys. Lett. B* **446**, 22 (1999).
12. K. Nomura, R. Rodríguez-Guzmán, L.M. Robledo. Shape evolution and the role of intruder configurations in Hg isotopes within the interacting boson model based on a Gogny energy density functional. *Phys. Rev. C* **87**, 064313 (2013).
13. C. Bernardis *et al.* Investigation of  $0^+$  states in  $^{198}\text{Hg}$  after two-neutron pickup. *Phys. Rev. C* **87**, 024318 (2013).
14. J.E. García-Ramos, K. Heyde. Disentangling the nuclear shape coexistence in even-even Hg isotopes using the interacting boson model. arXiv:1410.2869 (2014).
15. N. Bree *et al.* Shape coexistence in the neutron-deficient even-even  $^{182-188}\text{Hg}$  isotopes studied via Coulomb excitation. *Phys. Rev. Lett.* **112**, 162701 (2014).
16. J.M. Boillos, P. Sarriguren. Effects of deformation on the  $\beta$ -decay patterns of light even-even and odd-mass Hg and Pt isotopes. *Phys. Rev. C* **91**, 034311 (2015).
17. H.H. Kassim, F.I. Sharrad. Energy levels and electromagnetic transition of  $^{190-196}\text{Pt}$  nuclei. *Int. J. Mod. Phys. E* **23**, 1450070 (2014).
18. H.H. Kassim, F.I. Sharrad. High-spin structure in  $^{192-196}\text{Pt}$  isotopes. *Research & Reviews: J. of Phys.* **3**, 11 (2014).
19. H.H. Kassim, F.I. Sharrad.  $O(6)$  symmetry of even  $^{186-198}\text{Pt}$  isotopes under the framework of interacting boson model (IBM-1). *Int. J. of Sci. and Research (IJSR)* **3**, 2189 (2014).
20. F.I. Sharrad, H.Y. Abdullah, N. AL-Dahan, N.M. Umran, A.A. Okhunov, H. Abu-Kassim. Low-lying states of  $^{184}\text{W}$  and  $^{184}\text{Os}$  nuclei. *Chinese Phys. C* **37**, 034101 (2013).
21. F.I. Sharrad, H.Y. Abdullah, N. AL-Dahan, A.A. Mohammed-Ali, A.A. Okhunov, H.A. Kassim. Shape transition and collective excitations in neutron-rich  $^{170-178}\text{Yb}$  nuclei. *Rom. J. Phys.* **57**, 1346 (2012).
22. H.H. Khudher, A.K. Hasan, F.I. Sharrad. Calculation of energy levels, transition probabilities, and potential energy surfaces for  $^{120-126}\text{Xe}$  even-even isotopes. *Ukr. J. Phys.* **62**, 152 (2017).
23. F. Iachello, A. Arima. *The Interacting Boson Model* (Cambridge Univ. Press, 1987) [ISBN: 978-0521302821].
24. R.F. Casten, D.D Warner. The interacting boson approximation. *Rev. Mod. Phys.* **60**, 389 (1988).
25. F. Iachello, P. Van Isacker. *The interacting Boson Model* (Cambridge Univ. Press, 1991) [ISBN: 978-0521380928].
26. <http://www.nndc.bnl.gov/chart/getENSDFdatasets.jsp>.
27. B.J. Singh. Nuclear data sheets for  $A = 190$ . *Nucl. Data Sheets* **99**, 275 (2003).
28. C.M. Baglin. Nuclear data sheets for  $A = 192$ . *Nucl. Data Sheets* **84**, 717 (1998).
29. B.J. Singh. Nuclear data sheets for  $A = 194$ . *Nucl. Data Sheets* **107**, 1531 (2006).
30. H. Xiaolong. Nuclear data sheets for  $A = 196$ . *Nucl. Data Sheets* **108**, 1093 (2007).
31. H. Xiaolong. Nuclear data sheets for  $A = 198$ . *Nucl. Data Sheets* **110**, 2533 (2009).

Received 24.04.17

K.A. Хуссейн, М.К. Мохсин, Ф.І. Шаррад

РОЗРАХУНОК ІРАСТ-СМУГ  
З ПОЗИТИВНОЮ ПАРНІСТЮ ДЛЯ ЯДЕР  $^{190-198}\text{Hg}$ 

Резюме

Модель взаємодіючих бозонів (МВБ-1) застосовано для розрахунку низьколежачих іраст-смуг з позитивною парністю в  $^{190-198}\text{Hg}$  ядрах. Систематичний іраст-рівень і наведені ймовірності електричних переходів  $V(E2) \downarrow$  для цих ядер розраховані і порівнюються з експериментальними даними. Вивчено відношення  $R_{4/2}$  енергій збудження перших  $4^+$  і  $2^+$  порушених станів для  $O(6)$  симетрії. Для кількісної характеристики еволюції систематично досліджено іраст-рівень  $R = E_{L_1^+}/E_{2_1^+}$  деяких низьколежачих квадрупольних колективних станів і проведено порівняння з експериментом. Визначено систематичні  $V(E2)$  величини. Момент інерції як функція квадрата обергальної енергії ядер з парним числом протонів  $Z = 80$  і  $110 \leq N \leq 118$  свідчить про зникнення властивості зворотного вигину. Результати розрахунків знаходяться в хорошій відповідності з експериментом. Виконано аналітичний розрахунок іраст-рівня і  $V(E2)$  величин для парно-парних Hg ядер в рамках МВБ-1 і  $O(6)$  симетрії. Графіки поверхонь потенціальної енергії показують, що ядра деформовані і  $\gamma$ -нестабільні.